

# PREDICTION OF FLUID FLOW AND HEAT TRANSFER CHARACTERISTICS BEHIND A SINGLE BACKWARD-FACING STEP

A.K.M. Sadrul Islam and S. Ahmed

Department of Mechanical Engineering  
Bangladesh University of Engineering and Technology  
Dhaka - Bangladesh

**Abstract** Numerical solutions based on standard finite volume method are presented for the study of heat transfer and fluid dynamic characteristics in turbulent flows behind a single sided backward-facing step. The calculation of the differential equations is performed using SIMPLE algorithm. For the turbulent quantities standard  $k-\epsilon$  model is used. Predicted mean velocity profiles and reattachment lengths comply with the experimental data but significant deviation occurs in the predictions of turbulent intensities. The predicted heat transfer coefficient is in good agreement up to the reattachment point and downstream of that point it matches qualitatively.

چکیده برای مطالعه مشخصه‌های انتقال گرما و دینامیک شار در شارشهای متلاطم در پشت یک پله رو به عقب، راه حل عددی بر پایه روش متعارف حجم محدود ارائه شده است. محاسبه معادله دیفرانسیل با استفاده از الگوریتم ساده انجام شده است. در مورد کمیت‌های متلاطم، مدل متعارف  $k-\epsilon$  به کار رفته است. نمودار سرعت میانگین پیش‌گویی شده و طول برخورد مجدد با داده‌های تجربی می‌خوانند ولی خطای مهمی در پیش‌گویی شدت‌های متلاطم اتفاق می‌افتد. تا نقطه برخورد مجدد، ضریب انتقال گرمای پیش‌گویی شده در تطابق خوبی با داده‌های تجربی است و در پایین دست (پایاب) آن نقطه از لحاظ کیفی همساز می‌کند.

## INTRODUCTION

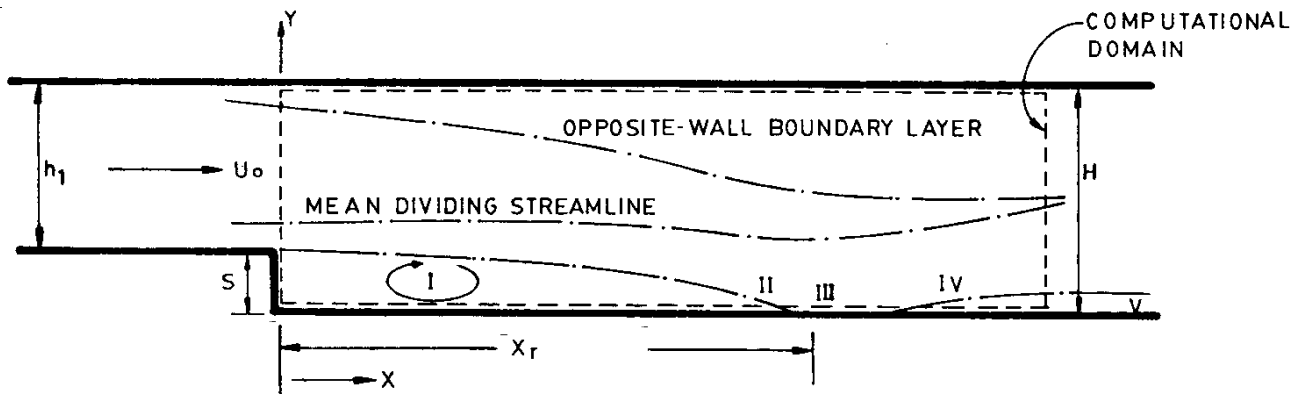
The reattachment of a shear layer, laminar or turbulent, has been the subject of study for many years because of its practical importance. These studies have attempted to explain the basic physics underlying the fluid dynamics and heat transfer behavior in the separated and reattaching shear layer. The heat transfer is intimately coupled with the fluid dynamics in reattaching flows. In a large number of practical heat transfer devices such as heat exchangers, turbine engines, electronic circuitry and nuclear reactors reattaching boundary layers can cause unexpected augmentation in the local heat transfer rate. This fact is creating great interest in numerical modeling of both the fluid dynamics and the heat transfer in a reattaching flow.

Among two dimensional flows the backward facing step is the simplest reattaching flow. This geometry fixes the point of separation, allows a spatially fixed free shear layer and incorporates a relatively easily located reattachment zone and redevelopment region (Figure 1). In addition the streamlines are nearly parallel to the wall at the separation point, so the principal elliptic interaction occurs downstream of separation.

The heat transfer process is intimately coupled with the fluid dynamics in reattaching flows. The heat transfer is

generally low in the recirculation region where velocities are less than the freestream. It then rises very rapidly approaching the reattachment region, where it peaks at values typically twice than under ordinary boundary layers. Downstream of reattachment, the heat transfer rate reduces back to the flat plate value.

In the last few years, there has been extensive work on the fluid dynamics of the backward-facing step. Eaton and Johnston [4] provided a comprehensive review of reattaching turbulent flow. Fletcher et al. [5], Aung and Watkins [2], Vogel and Eaton [12] have also included a survey of heat transfer experiments in reattachments. The prediction of heat transfer rates in such cases is not yet successful. The main reason for this is the treatment of the wall boundary condition. Chieng and Launder [3] predicted the heat transfer rates downstream of an abrupt pipe expansion using the standard  $k-\epsilon$  model with wall function proposed by Jayatileke [6] and this leads to a result of heat transfer rates within 15% of the experimental values. Amano [1] improved the prediction of mean heat transfer rate in pipe expansion using a modified  $k-\epsilon$  model but underestimated the location of maximum heat transfer point by 30-50%. In these predictions, the governing differential equations were discretised by UPWIND and central difference schemes.



I BACKFLOW ZONE II SEPARATED SHEAR LAYER III REATTACHMENT ZONE  
IV REDEVELOPING NEAR-WALL FLOW V RELAXING OUTER SHEAR LAYER

Figure 1. Schematic of the Single-Sided Backward-Facing Step

The objective of the present study was to predict the fluid dynamic and heat transfer characteristics behind a single sided backward-facing step using the standard  $k-\epsilon$  model incorporating the third order accurate quadratic discretization scheme of the governing equations. For heat transfer calculations, Jayatilke's wall function was used [6]. The calculated results were compared with the measurements of Eaton and Jonston [4] and Vogel and Eaton [11, 12].

#### MATHEMATICAL MODEL AND COMPUTATIONAL DETAILS

The predictions were obtained by numerical solution of the

time-mean equations governing conservation of mass, momentum and the scalar enthalpy equation, supplemented by a two-equation ( $k-\epsilon$ ) effective viscosity turbulence model. The general form of the equations for steady incompressible turbulent flow in Cartesian geometry is:

$$\frac{\partial}{\partial x_i} (\rho U_i \phi) = \frac{\partial}{\partial x_i} (\Gamma_\phi \frac{\partial \phi}{\partial x_i}) + S_\phi \quad (1)$$

where  $\phi$  represents one of the dependent variables  $U, V, K, \epsilon$  and  $\theta$ . The turbulent exchange coefficients,  $\Gamma_\phi$ , and source terms,  $S_\phi$  for each dependent variable are given in Table 1.

TABLE 1. The Conservation Equations

Equation	$\phi$	$\Gamma_\phi$	$S_\phi$
Mass	1	0	0
U-momentum	U	$\mu_{eff}$	$-\frac{\partial P}{\partial X} + \frac{\partial}{\partial X} (\mu_{eff} \frac{\partial U}{\partial X}) + \frac{\partial}{\partial Y} (\mu_{eff} \frac{\partial U}{\partial Y})$
V-momentum	V	$\mu_{eff}$	$-\frac{\partial P}{\partial Y} + \frac{\partial}{\partial X} (\mu_{eff} \frac{\partial V}{\partial X}) + \frac{\partial}{\partial Y} (\mu_{eff} \frac{\partial V}{\partial Y})$
Enthalpy	$\theta$	$\frac{\mu}{\sigma_\theta} + \frac{\mu_t}{\sigma_{\theta,t}}$	0
Turbulent kinetic energy	k	$\frac{\mu_{eff}}{\sigma_k}$	G - $\rho\epsilon$
Dissipation of k	$\epsilon$	$\frac{\mu_{eff}}{\sigma_\epsilon}$	$-\frac{\epsilon}{k} (C_1 G - C_2 \rho\epsilon)$

$$\mu_{eff} = \mu + \mu_t, \mu_t = C_\mu \rho k^2 / \epsilon$$

$$G = \frac{\mu_{eff}}{\rho} \{ 2 [ (\frac{\partial U}{\partial X})^2 + (\frac{\partial V}{\partial Y})^2 ] + (\frac{\partial U}{\partial Y} + \frac{\partial V}{\partial X})^2 \}$$

$C_\mu$	$C_1$	$C_2$	$\sigma_k$	$\sigma_\epsilon$	$\sigma_\theta$	$\sigma_{\theta,t}$
0.09	1.44	1.92	1.0	1.3	0.72	0.9

The boundary conditions were obtained from the measurements wherever possible. Thus, the inlet velocities and turbulence levels were taken from the measurements at the point of separation. The turbulent energy dissipation rate at the point of separation was estimated from an assumed mixing length:

$$\epsilon_o = k_o^3 / l \quad (2)$$

Where  $l$  was taken as the channel inlet depth,  $h_1$ . At the outflow boundary, which was located beyond the reattachment point in the redevelopment region (say at  $X/S = 30$ ), the  $V$  velocity was set to zero and streamwise derivatives of  $U$  velocity, turbulent kinetic energy, turbulent energy dissipation rate and temperature were set to zero. At solid surfaces the velocities were set to zero and so-called wall functions, based on logarithmic velocity profiles, were used to bridge the turbulent boundary layer.

$$U^+ = \frac{1}{\kappa} \ln(Ey^+) \quad (3)$$

$$\frac{\partial k}{\partial Y} = 0 \quad (4)$$

$$\epsilon_p = C_\mu^{3/4} k_p^{3/2} / (\kappa y) \quad (5)$$

Where,

$$y^+ = (C_\mu^{1/4} \rho k_p^{1/2} / \mu) y$$

$$U^+ = (C_\mu^{1/4} \rho k_p^{1/2} / \tau_w) U_p$$

and  $U_p$  is the velocity parallel to the wall,  $\tau_w$  the shear stress at the wall and  $y$  the normal distance from the wall.

The interlinkage between the near-wall variation in temperature and the local wall heat flux was obtained from Chieng and Launder [3]:

$$T_p = T_w + \frac{q''}{\rho C_p k_p^{1/2}} \left\{ \rho U_p \frac{k_p^{1/2}}{\tau_w} + f(\sigma) \right\} \quad (6)$$

where  $C_p$  is the specific heat at constant pressure and the function  $f(\sigma)$  was taken from Jayatilke [6]:

$$f(\sigma) = 9.0 \left[ \left( \frac{\sigma_{\theta}}{\sigma_{\theta,t}} \right)^{0.75} - 1.0 \right] \left[ 1.0 + 0.28 \exp(-0.007 \frac{\sigma_{\theta}}{\sigma_{\theta,t}}) \right]$$

For a Prandtl number of 0.72 appropriate to the air-flow cases considered, the  $f(\sigma)$  takes the value of -1.77.

The differential equations were reduced to a conserva-

tive finite difference form using the control-volume method over a rectangular grid covering the flow domain (Figure 1). Staggered grids were employed for the  $U$  and  $V$  equations. The pressure and scalar quantities were located at the grid nodes. A third order accurate QUICK scheme of Leonard [8] was used for discretization of the convective terms whereas the diffusive fluxes and the source terms were discretized using second order accurate central differencing. The use of QUICK scheme reduces numerical inaccuracies due to false diffusion related to the first order UPWIND scheme [7, 9]. The finite difference equations were solved simultaneously using the SIMPLE algorithm of Patankar and Spalding [10] by repeated sweeps of a line by line application of Tri-diagonal Matrix Algorithm. Since the mass and momentum equations are not coupled with temperature, the enthalpy (temperature) equation was solved after the convergence of the momentum equations.

The final computations were carried out on a nonuniform  $40 \times 25$  ( $x, y$ ) grid with a concentration of nodes within the expected recirculation region. The results were checked for grid independence within reasonable limits, by comparison with results obtained on a  $30 \times 14$  grid. The differences in the calculated velocities were typically less than five percent of the maximum velocity. The grid dependence, clearly non-zero, is small and no further grid refinement was possible due to the limitation of the computer resources. The calculations were carried out on an IBM PS-2/50 computer in the Department of Mechanical Engineering, BUET.

## RESULTS AND DISCUSSION

In the present prediction both fluid dynamics and heat transfer characteristics of recirculating reattaching flow were investigated and compared with the experimental data.

The prediction of turbulent recirculating reattaching flow for three different Reynolds numbers based on step height ( $Re_s = 11,000, 28,000$  and  $40,000$ ) is presented. The experimental data for Reynolds numbers 11,000 & 40,000 are taken from Eaton and Johnston [4] and for 28,000 from Vogel and Eaton [11]. In the two former cases, only fluid dynamic data are available, whereas in the latter case relevant heat transfer data are also found.

### Fluid Dynamic Characteristics

Vogel and Eaton [11] measured the reattachment length ( $X_r$ ) by taking the distance from the backward-facing step face to the point of zero mean skin friction coefficient, corresponding to the point of 50% forward flow fraction. The 50% forward flow fraction is defined as the point at which the flow is going upstream half the time and downstream the other half according to the definition of Westphal [13]. In the present prediction this length is taken as the

distance of zero stream function line from step face along the lower wall which corresponds to the point of zero mean skin friction coefficient. The predicted and measured values of  $(X_r)$  are presented in Table 2. The prediction of reattachment lengths is in good agreement with the experimental values.

**TABLE 2. Reattachment Length of Turbulent Flows**

$Re_s$	Expansion ratio $H/h_1$	$(X_r)/S$		Reference of measurement
		Present prediction	Measured	
11,000	1.67	7.6	6.97	Eaton & Johnston, [4]
28,000	1.25	6.95	6.68	Vogel & Eaton, [11]
40,000	1.67	7.72	7.95	Eaton & Johnston, [4]

Mean-velocity profiles for all three cases are shown in Figures 2 through 4. The velocity profiles show the shear layer growing by entrainment as it proceeds downstream and then intercepting the wall at the reattachment point. Underneath the shear layer, the near-wall boundary layer starts near reattachment point and flows upstream towards the step. The predicted mean velocity profile agrees quite well with the experimental one but slight deviation occurs in the downstream of reattachment. The maximum backflow velocity found in the present prediction is about 24% of the freestream velocity which is very close to the experimental value of 20% [12]. The location of maximum backflow velocity is about 0.1 step height from the wall and about 3.5 to 4.0 step height downstream of the step face.

Figures 5 through 7 present the fluctuating component of the streamwise velocity for the three Reynolds number cases. The peak intensity grows and the region of turbulence broadens as the shear layer develops. The turbulence intensity then decays, beginning near the reattachment zone. The location of the peak in the turbulence intensity profiles starts at about  $Y/S = 1.0$  downstream of separation. The peak dips down towards the wall in the recirculating zone and then moves back out towards  $Y/S = 1.0$  downstream of reattachment (not shown in the figure).

In the present prediction the trend of the turbulent normal stress profiles is similar to that of the experiment. The maximum underprediction is about 50% which occurs near the step edge for all cases. The predicted profiles gradually approach that of the experiment in the reattachment zone and then about 15% overprediction occurs far downstream of reattachment zone (Figure 6). The peak level of  $u'$  for  $Re_s = 28,000$ , around 14.5%

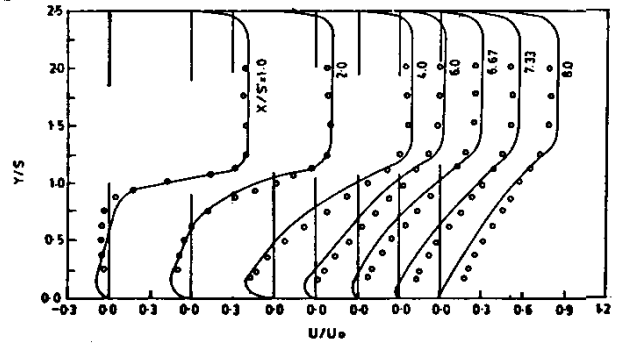


**Figure 2. Mean Velocity Profiles at Different Axial Locations for  $Re_s = 11000$**   
— Present Prediction, o Expt. (Eaton & Johnston, 1980)

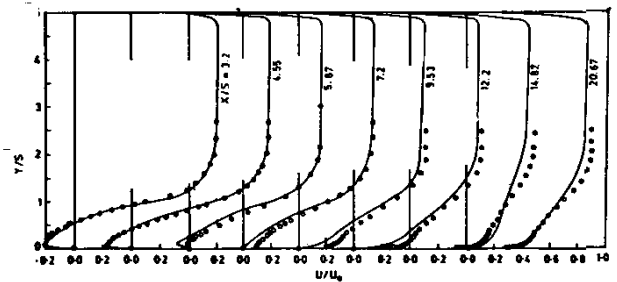


**Figure 3. Mean Velocity Profiles at Different Axial Locations for  $Re_s = 28,000$**   
— Present Prediction, o Expt. (Vogel and Eaton, 1984)

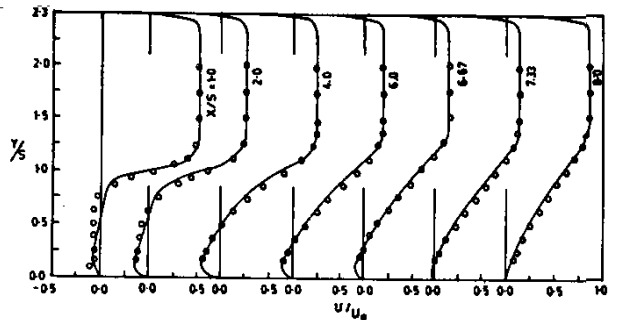


**Figure 4. Mean Velocity Profiles at Different Axial Locations for  $Re_s = 40000$**   
— Present Prediction, o Expt. (Eaton & Johnston, 1980)

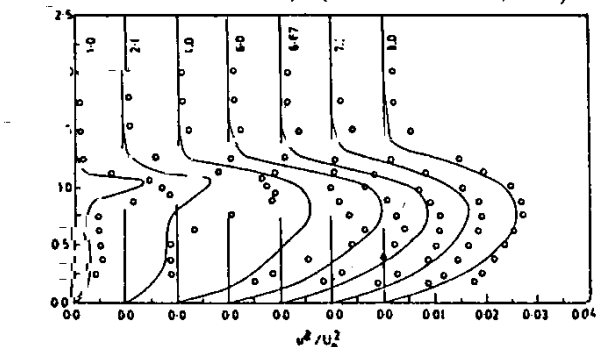


**Figure 5. Turbulent Normal Stress Profiles at Different Axial Locations for  $Re_s = 11000$**   
— Present prediction, o Expt. (Eaton & Johnston, 1980)

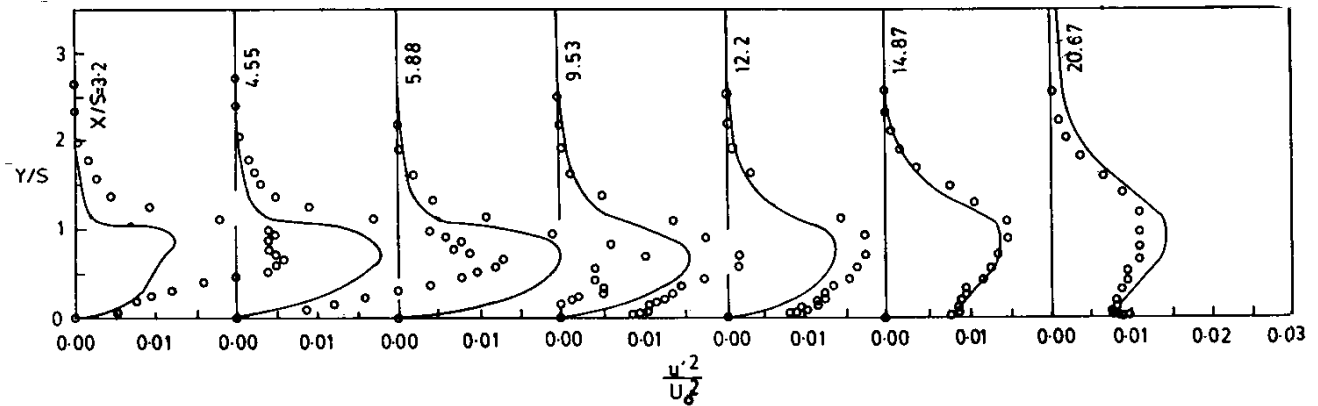


Figure 6. Turbulent Normal Stress Profiles at Different Axial Locations for  $Re_s = 28000$  — Present Prediction, o Expt. (Vogel and Eaton, 1984).

normalized on the freestream velocity, is found in the recirculation region at  $X^* = -0.12$  ( $X/S = 5.88$ ) whereas in the experiment [12], the peak level and location were 18% and at  $X^* = -0.32$  ( $X/S = 4.55$ ), respectively.

### Heat Transfer Characteristics

Figure 8 shows the Stanton number variation for the Reynolds number cases considered here. Constant heat flux ( $q''_w = 130 \text{ W/m}^2$ ) boundary condition is assumed at the step wall according to the experimental setup of Vogel and Eaton [11, 12].

All of the Stanton number profiles have the same general features. There is a low heat transfer rate in the recirculation region ( $X^* < 0$ ), followed by a steep rise to a maximum near the reattachment point. By comparing the location of the reattachment point to the location of the peak heat transfer rate, Vogel and Eaton [11] found that the maximum occurs slightly upstream of the reattachment. In the present prediction it is found that the maximum Stanton number occurs at about  $0.13 X^*$  to  $0.17 X^*$  upstream of reattachment point depending on the Reynolds number, whereas the experimental value was at about  $0.1 X^*$  upstream for  $Re_s = 28,000$ . The heat transfer rate then declines

by 40% to 50% from the peak value depending on the Reynolds number, downstream of reattachment, to a typical flat-plate level.

Figure 9 shows that normalizing the reference Stanton number profile on the maximum value of Stanton number collapsed almost to one profile although there is slight deviation downstream of reattachment. The experimental data of Vogel and Eaton [11] for  $Re_s = 28,000$ , is identical with the predicted profile up to the reattachment point and then deviates considerably.

The predicted mean temperature profiles for  $Re_s = 28,000$  are presented in Figure 10 for various streamwise locations downstream of the separation. The temperature profiles show the steepest temperature gradients, and therefore most of the thermal resistance, in the region very close to the wall, which is conduction dominated. Only in one of the profiles, that closest to the step at  $X/S = 0.33$ , is there a significant temperature gradient in the flow far from the wall, most of it across the free shear layer. This gradient also exists for  $X/S = 1.66$  but gradually decreases and almost diminishes after reattachment. The predicted profiles deviate considerably in the recirculation region

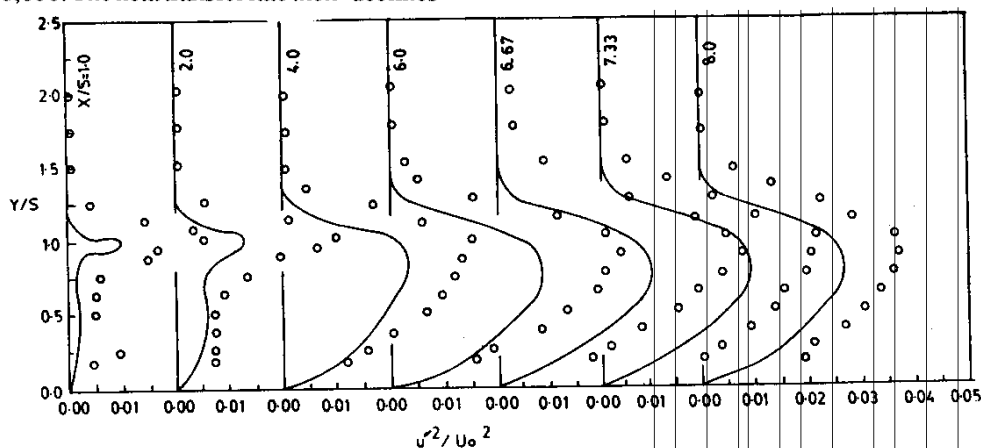


Figure 7. Turbulent Normal Stress Profiles at Different Axial Locations for  $Re_s = 40000$  — Present Prediction, o Expt. (Eaton & Johnston, 1980).

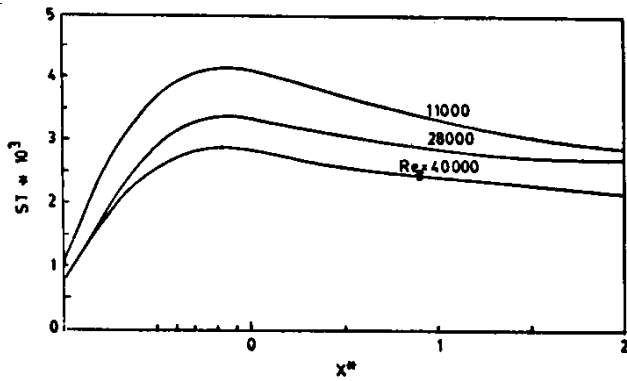


Figure 8. Stanton Number Variations for Different Reynolds Number

and after reattachment point ( $X/S > 6.7$ ), these are close to the experimental data. This deviation is due to the shortcomings of the diffusion modeling of temperature equation. Greater convective mixing effects in the other regions of the flow do not allow steep temperature gradients except near the wall and across the shear layer near the separation. The temperature drop across the shear layer suggests that the warmer slow-moving recirculation fluid is not rapidly transported across the recently separated shear layer.

### CONCLUSION

The main conclusions of this study may be summarized as follows:

1. The turbulent model predicts the mean velocity profile relatively accurately for the range of Reynolds numbers considered here, although there are small deviations in the profiles after reattachment point. Prediction of magnitude and location of maximum backflow velocity is fairly good.
2. Prediction of turbulent fluctuating component is not

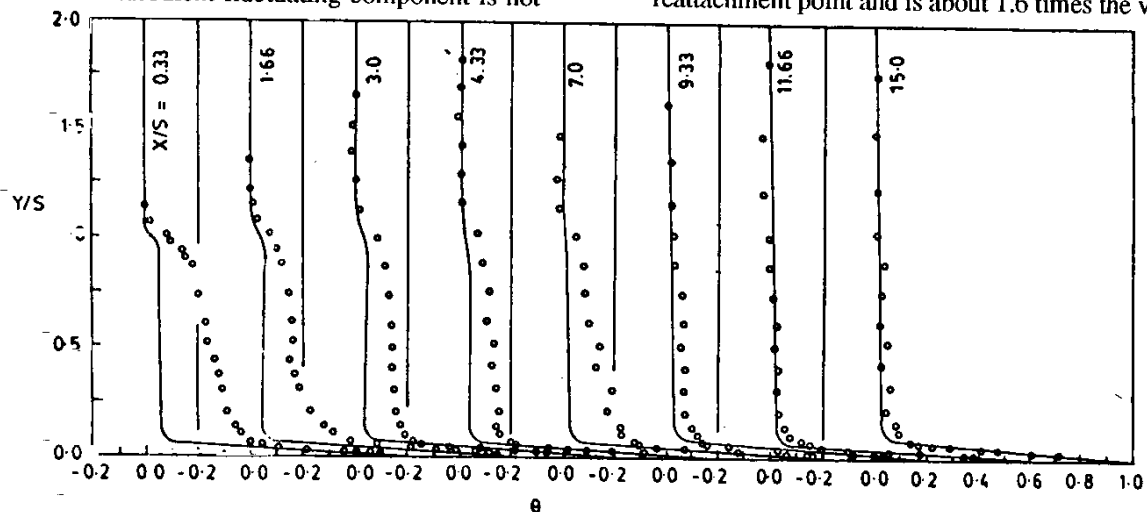


Figure 10. Temperature Profiles at Different Axial Locations for  $Re_s = 28000$   
 o Expt. (Vogel and Eaton, 1984).

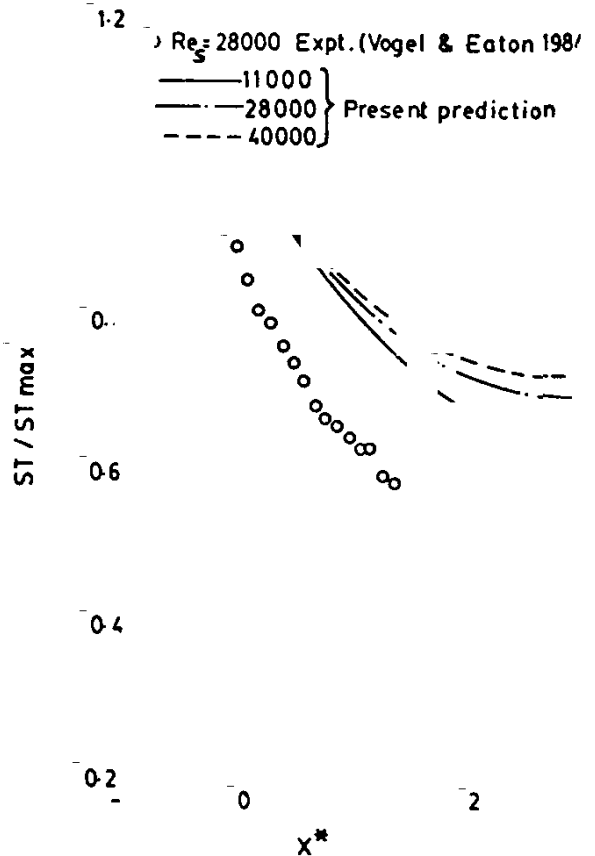


Figure 9. Stanton Number Profiles Varying with Reynolds Number Normalized on the Maximum Stanton Number

very good. There is under-prediction of about 50% in the maximum turbulent normal stress near the separation point. The difference gradually decreases and close to the reattachment point, prediction approaches experimental data.

3. The peak heat transfer coefficient occurs around the reattachment point and is about 1.6 times the value at

a downstream location. The maximum heat transfer rate lies from  $0.13 X^*$  to  $0.17 X^*$  upstream of reattachment point depending on the Reynolds number.

- The temperature profiles show the steepest gradients in the region very close to the wall which is conduction dominated. There is a significant temperature drop across the shear layer in the recirculation region. The temperature profiles in the upstream of reattachment cannot be predicted with accuracy due to the shortcomings of the diffusion modeling of temperature equation.

#### Nomenclature:

$C_p$	Specific heat
$h$	Heat transfer coefficient, $q''_o / (T_w - T_o)$
$h_1$	Channel height, $h_1 + S$
$k$	Turbulent kinetic energy, $u'^2/2$
$P$	Pressure
$q''_o$	Wall heat transfer rate per unit area
$Re_s$	Reynolds number based on step height, $U_o S / \nu$
$S$	Step height
$ST$	Stanton number, $h / U_o C_p \rho$
$T$	Local mean temperature
$T_o$	Free stream temperature
$T_w$	Local wall temperature
$U_o$	Free stream velocity
$U$	Mean streamwise velocity
$u'$	Fluctuating streamwise velocity
$V$	Mean normal velocity
$v'$	Fluctuating normal velocity
$X$	Streamwise distance from step edge
$X_1$	Reattachment length from step edge
$X^*$	Non-dimensional reattachment length, $(X - X_1) / X_1$
$Y$	Distance from the step wall

#### Greek Letters:

$\nu$	Freestream kinematic viscosity
$\theta$	Non-dimensional local temperature difference, $(T - T_o) / (T_w - T_o)$
$\rho$	Density

$\mu$	Viscosity
$\sigma$	Prandtl number
$\sigma_t$	Turbulent Prandtl number for heat transfer
$\epsilon$	Turbulent energy dissipation rate
$K$	Constant in logarithmic velocity profile

#### REFERENCES

- R. Amano *AIAA Journal* 21, 1400-1405 (1983).
- W. Aung and C.B. Watkins "Heat Transfer Mechanism in Separated Forced Convection", Proc. of the NAT Inst on Turbulent Forced Convection in Channels and Bundles; Theory and Application to Heat Exchangers, Turkey, June 20-Aug. 2 (1978).
- C.C. Chieng and B.E. Launder. *Numerical Heat Transfer* 3, 189-207 (1987).
- J.K. Eaton and J.P. Johnston "Turbulent Flow Reattachment: An Experimental Study of the Flow and Structure Behind a Backward-Facing Step". Report MD-39, Stanford University, Stanford, CA, 94305, June (1980).
- L.S. Fletcher, D.G. Briggs and R.H. Page, *Israel J. of Tech.* 12, 236-361 (1974).
- C.C.V. Jayatilake *Prog. Heat and Mass Transfer*, 1, 193-329 (1969).
- B.P. Leonard, M.A. Leschziner and J. J. McGuirk "Third Order Finite-Difference Method for Steady Two-Dimensional Convection", Numerical Methods in Laminar and Turbulent Flows, (C. Taylor et al. Ed.), Pentach, London, England (1978).
- B.P. Leonard, *Comp. Methods in Appli. Mech. and Eng.* 19, 59-98 (1979).
- M.A. Leschziner and W. Rodi. *J. Fluid Engg.*, ASME. 103, 352-360 (1981).
- S.V. Patanker and D.B. Spalding, *Int. J. Heat and Mass Transfer*, 15, 1787-1806 (1972).
- J.C. Vogel and J.K. Eaton. *J. of Heat Transfer*, ASME. 107, 922-929 (1985).
- J.C. Vogel and J.K. Eaton, "Heat Transfer and Fluid Mechanical Measurements in the Turbulent Reattaching Flow Behind a Backward Facing Step". Report MD-44, Thermosciences Division, Dept. of Mechanical Engineering, Stanford University, July (1984).
- R. Westphal "Experimental Study of Flow Reattachment in a Singlesided Sudden Expansion" Ph.D. Dissertation, Dept. of Mechanical Engineering, Stanford University, USA (1982).